Continental Shelf Research 124 (2016) 165–181

Contents lists available at ScienceDirect

Continental Shelf Research

journal homepage: www.elsevier.com/locate/csr

Research papers

Surface and bottom temperature and salinity climatology along the continental shelf off the Canadian and U.S. East Coasts

Benjamin Richaud [a,b], Young-Oh Kwon [a,*], Terrence M. Joyce [a], Paula S. Fratantoni [c], Steven J. Lentz [a]

[a] Woods Hole Oceanographic Institution, Woods Hole, MA, USA
[b] ENSTA ParisTech, Palaiseau, France
[c] NOAA/NMFS, Northeast Fisheries Science Center, Woods Hole, MA, USA

ARTICLE INFO

Article history:
Received 4 June 2015
Received in revised form
2 April 2016
Accepted 12 June 2016
Available online 15 June 2016

Keywords:
Seasonal climatology
Temperature
Salinity
Dataset
Shelf

ABSTRACT

A new hydrographic climatology has been created for the continental shelf region, extending from the Labrador shelf to the Mid-Atlantic Bight. The 0.2-degree climatology combines all available observations of surface and bottom temperature and salinity collected between 1950 and 2010 along with the location, depth and date of these measurements. While climatological studies of surface and bottom temperature and salinity have been presented previously for various regions along the Canadian and U.S. shelves, studies also suggest that all these regions are part of one coherent system. This study focuses on the coherent structure of the mean seasonal cycle of surface and bottom temperature and salinity and its variation along the shelf and upper slope. The seasonal cycle of surface temperature is mainly driven by the surface heat flux and exhibits strong dependency on latitude ($r \approx -0.9$). The amplitude of the seasonal cycle of bottom temperature is rather dependent on the depth, while the spatial distribution of bottom temperature is correlated with latitude. The seasonal cycle of surface salinity is influenced by several components, such as sea-ice on the northern shelves and river discharge in the Gulf of St. Lawrence. The bottom salinity exhibits no clear seasonal cycle, but its spatial distribution is highly correlated with bathymetry, thus Slope Water and its intrusion on the shelf can be identified by its relatively high salinity compared to shallow, fresher shelf water. Two different regimes can be identified, especially on the shelf, separated by the Laurentian Channel: advection influences the phasing of the seasonal cycle of surface salinity and bottom temperature to the north, while in the southern region, river runoff and air-sea heat flux forcing are dominant, especially over the shallower bathymetry.

1. Introduction

It would be an euphemism to say that the Canadian and U.S. East Coast are an important area for fisheries. Considering how European fishermen used to cross the Atlantic Ocean to confront the mists of the Grand Banks and the marks that their often tragic epics left in literature (Kipling, 1897; Loti, 1886), the impact of the region in history and science is not to be underestimated. Accordingly, numerous previous studies examined the oceanography of the individual regions along the continental shelf from the Mid-Atlantic Bight to the Labrador Sea. Yet, a relatively limited number of studies have tried to understand the links between these regions, or considered the eastern shelf as one coherent system.

The temperature, salinity, depth and width of the continental shelf all vary considerably along the approximately 5000 km distance between Labrador and Cape Hatteras, posing a significant challenge to examining the climatology in a coherent fashion. The Labrador Shelf is partly or completely covered by sea-ice from December to June (see the red contour in the Fig. 1 for maximum extent of the 15% sea-ice concentration). The maximum extent of ice coverage is reached in February or March, and the ice, pushed southward by both the wind-driven and the buoyancy-driven circulations, is found as far south as 45°N, covering most of the Newfoundland Shelf and the Gulf of St. Lawrence (Ikeda et al., 1996; National Snow and Ice Data Center, 2006). This sea-ice insulates the shelf water from atmospheric forcing and thus alters the variability of temperature and salinity on the Labrador Shelf, and also in the Gulf of St. Lawrence from January to April. This is not the case in the Mid-Atlantic Bight, where waters never reach freezing temperatures. Bathymetry also encourages a more

* Correspondence to: Physical Oceanography Department, Woods Hole Oceanographic Institution, Woods Hole, MA 02543, USA.
E-mail address: yokwon@whoi.edu (Y.-O. Kwon).

http://dx.doi.org/10.1016/j.csr.2016.06.005
0278-4343/

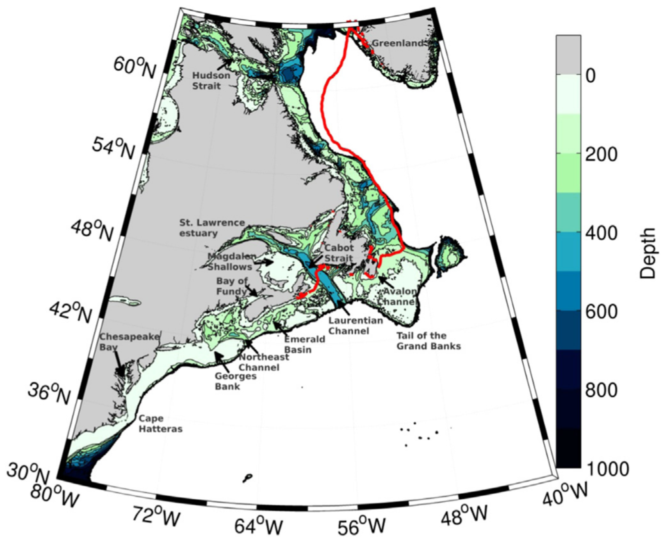

Fig. 1. Bathymetry of the study area. Contours are given every hundred meters from 0 to 1000 m. The red line shows the maximum 15% concentration sea-ice extent. (For interpretation of the references to color in this figure legend, the reader is referred to the web version of this article.)

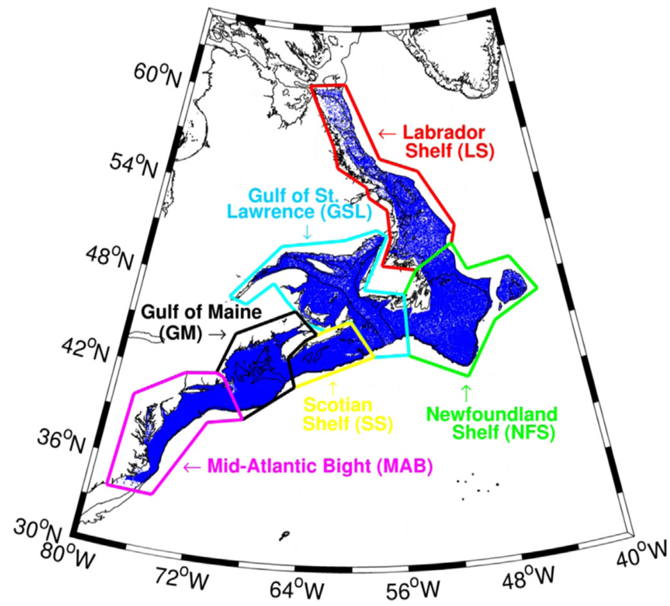

Fig. 2. Description of the six sub-regions. Each data point is represented by a blue dot. Contours represent the 0, 200 and 600 m isobaths. (For interpretation of the references to color in this figure legend, the reader is referred to the web version of this article.)

regional focus, with the shelf break shoaling from 300 m in the north to 50 m in the south, the 500 m deep Laurentian Channel bisecting the shelf just west of the Grand Banks, and with the shallow, open Grand Banks of Newfoundland contrasting the deep, enclosed basins of the Gulf of Maine.

Despite these regional differences, Chapman and Beardsley (1989) have used oxygen isotope measurements to demonstrate the interconnected nature of the coastal circulation in the western North Atlantic, tracing the origin of the shelf water in the Mid-Atlantic Bight poleward to the southern coast of Greenland. Furthermore, Loder et al. (1998) discuss the circulation, transport, and hydrography of the northeastern North American coastal ocean as a single large-scale physical regime, predominantly influenced by this coastal boundary current system. Features of the shelfbreak front, where cooler fresher shelf water meets warmer saltier Slope Water, exhibit similar large-scale continuity. The examination by Fratantoni and Pickart (2007) of over 700 synoptic hydrographic sections between the west coast of Greenland and the Mid-Atlantic Bight demonstrated a coherent evolution of both the structure of the front and its associated current.

The Baffin Current and the westward branch of the West Greenland Current converge on the northern Labrador Shelf to form the Labrador Current and its associated shelf flow (see Figs. 1 and 2 for the map of study area ; also see the Figure 1 of Fratantoni and Pickart (2007)). While a large portion of this current recirculates into the subpolar gyre upon reaching the Grand Banks of Newfoundland (Fratantoni and McCartney, 2010), the rest follows the shelf equatorward, ultimately reaching the Mid-Atlantic Bight, where it encounters the Gulf Stream near Cape Hatteras (Fratantoni and Pickart, 2007). According to Loder et al. (1998), this circulation is driven by buoyancy. Since the Labrador Current is the western boundary current of the subpolar gyre and the Gulf Stream is the western boundary current of the subtropical gyre, our area of study is confined between two major gyres carrying contrasting water masses and is influenced by both. Snow and ice melts from Greenland and Hudson Strait area represent a significant source of fresh water to the coastal boundary current system on the Labrador Shelf, further combined with the St. Lawrence river runoff, to form the mean flow on the Scotian Shelf (Chapman and Beardsley, 1989; Khatiwala et al., 1999). Further south, freshwater input is predominantly from rivers and estuaries in the northern Gulf of Maine and southern Mid-Atlantic Bight. Fresh shelf water is mixed with saltier Slope Waters through various means, including vertical tidal mixing (Garrett and Loder, 1981), winter convective overturning (Mountain and Jessen, 1987), and as part of cross-shelf exchanges through deep channels such as the Laurentian and Northeast Channels (Galbraith, 2006; Mountain and Manning, 1994), as well as smaller channels cutting into the Scotian Shelf (Drinkwater and Gilbert, 2004).

Previous studies have shown that temperature and salinity at the surface and the bottom of the ocean exhibit coherent variability along the shelf over a range of timescales. Loder et al. (1998) emphasized this coherence on seasonal time scales based on maps and vertical sections of winter and summer temperature and salinity. On interannual timescales, Petrie (2007) reported a coherent structure of bottom temperature and salinity anomalies from the Labrador Shelf to the Gulf of Maine associated with the North-Atlantic Oscillation. Finally, Shearman and Lentz (2010) showed that century-long ocean warming trends observed along the entire northeast U.S. coast are not related to local atmospheric forcing but driven by atmospheric warming of source waters in the Labrador Sea and the Arctic, which are advected into the region.

The remainder of this paper is organized as follows. In Section 2, we describe the construction of the climatology, including data sources, quality control and gridding procedures. In Section 3, the mean seasonal cycles of surface/bottom temperature/salinity are described with focus on their latitudinal coherence and variation along the shelf and upper slope over the study region. More detailed examination of the specific regional patterns is presented in Section 4. The discussion and conclusion are given in Section 5.

2. Data

2.1. Sources

To obtain a coherent dataset over a large region, from Cape Hatteras to the Labrador Shelf, and over the longest possible time span, two different data sets were processed in an identical way and combined. The first one, the temperature and salinity from the

Canadian Ocean Science Hydrographic Climate Database,[1] includes observations from 1910 to 2010 along the Canadian Atlantic Shelf (Gregory, 2004) and is archived at the Bedford Institute of Oceanography. The second data set was extracted from the National Oceanographic Data Center in the United States,[2] and was augmented with old, hand-written observations (Bigelow, 1933) as well as temperature and salinity profiles collected by the Northeast Fisheries Science Center of the U.S. National Marine Fisheries Service, as described by Shearman and Lentz (2010). This database dates back to 1864, covering the U.S. Atlantic Shelf from Cape Hatteras to the Scotian Shelf, where it overlaps with the Canadian database.

From these two datasets, only surface and bottom temperature and salinity measurements were retained along with their location, date/time and observation depth. Data within the top 5 m of the water column are considered surface data, while those within ±10 m from the bottom are considered bottom data. Water depth is not consistently included in archives of oceanographic data, so we derive it using the geographic position of each observation and a 1-min resolution topography product, ETOPO1[3] (Amante and Eakins, 2009). Since we are primarily focused on the continental shelf and upper slope, only observations having bottom depths less than 600 m are retained. Similarly, only surface data are retained in areas where the water depth is shallower than 15 m, as the bottom and surface layers are not clearly separated according to our definition.

An outlier filter is applied to both datasets as a quality control on the data. Observations are binned into 0.5-degree latitude/longitude bins and a monthly mean and standard deviation is calculated for those bins/months where at least five observations are available. An observation is considered an outlier and removed if its difference from the local mean value is greater than 3 times the standard deviation. Following this, another filter is applied to avoid spatial and temporal clustering. A cluster is defined as multiple data points that have been collected within a 24 h period and 5 km radius. When a cluster of data is found, it is replaced by the mean value of the cluster.

Following the quality control filters, the two overlapping datasets were merged. Duplicated data were identified and removed in the overlapping region on the Scotian Shelf. In addition, the cluster filter described above was applied one more time in the overlapping region after the merge. The resulting merged database contains more than 403,000 stations, derived from a variety of sources, including CTD casts, profiling floats, and bathythermographs. Each station in the final dataset may include a combination of temperature and/or salinity at either the surface and/or the bottom.

The Canadian and U.S. east coast is divided into six regions for the analyses presented in the rest of this section (Fig. 2). The distribution of the stations is shown in Fig. 2, with relatively sparse coverage over the Labrador Shelf.

2.2. Temporal distribution

While the entire dataset spans nearly 150 years, the number of observations increases significantly beginning in the late 1940s for salinity and a bit earlier for temperature (Fig. 3). Thus, our analysis period is limited to 1950–2010. The number of surface observations is ~1.5 times larger than the number of bottom values for both temperature and salinity. It is noteworthy that a drop in the number of observations occurs after mid-2000. This may be due to

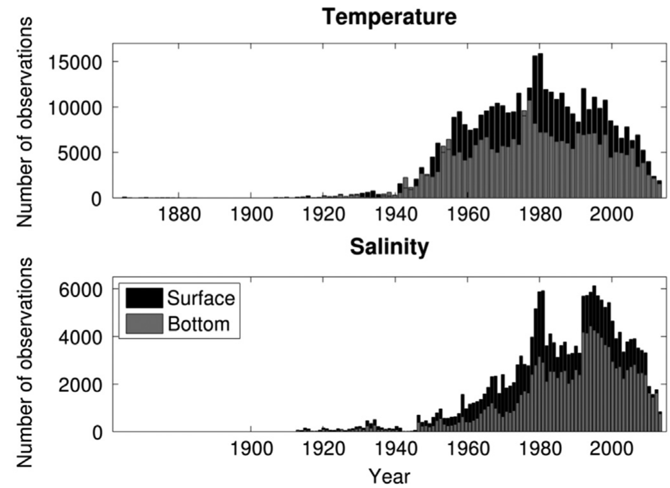

Fig. 3. Number of available observations per year. Black is for surface, while gray represents bottom observations for the temperature (top) and salinity (bottom).

the fact that more recent data have not yet been incorporated into the national archives. Data coverage is uneven among different geographic regions (as suggested in Fig. 2) and seasons. Generally, more data are available from the spring to fall and in the southern regions (Fig. 4). While the Mid-Atlantic Bight and the Gulf of Maine are reasonably sampled throughout the year, coverage is sparse on the Labrador Shelf, particularly during winter, probably due to harsh weather conditions and sea ice. Thus, results for this region will have to be interpreted with greater care.

2.3. Bin-average and gap-filling

Monthly climatologies are constructed for the period 1950–2010 by binning and averaging data within bins measuring $0.2 \times 0.2°$ in latitude and longitude. To avoid potential bias due to uneven sampling in time, the average was first calculated for every month of every year between 1950 and 2010. No threshold was defined to calculate the mean, i.e. even if only one observation was available for a specific month and year, it was considered as a mean.

To further minimize the bias associated with sparse temporal sampling, each grid (month, year, latitude, longitude) without an average is filled by extrapolation from the adjacent months. The process used to fill those gaps is schematically described in Fig. 5. First, the study area is divided into several large regions, sliding 5 degrees in latitude and spanning 20 m range in bathymetry as illustrated schematically in Fig. 6. A mean seasonal cycle is calculated from monthly averages of data collected between 1970 and 2010 within each of these regions and used as the reference for the region (black curve in Fig. 5). For each target grid with a missing value in a specific month and year, the slope from the mean seasonal cycle (blue bars in Fig. 5) is used to extrapolate the missing value from the known value in the adjacent month of the same year (red square in Fig. 5). If the temperature/salinity is known for both the preceding and following month, the mean of both inferred values is used in place of the missing point. If three or more consecutive months are missing, only the two missing values in the end points are filled using this method. While the mean seasonal cycles are calculated for a large region, extrapolations are done on the much smaller 0.2 degree grid.

The 20 m bathymetry range for the mean seasonal cycle is adopted to take into account the dominant along-shelf/along-slope coherence of salinity and temperature. As the mean seasonal cycle cannot be robustly defined for bottom temperature and salinity (as discussed further in Section 3), gap-filling is only

[1] Accessible at http://www.bio.gc.ca/science/data-donnees/base/data-donnees/climate-climat-eng.php
[2] http://www.nodc.noaa.gov
[3] http://www.ngdc.noaa.gov/mgg/global/global.html

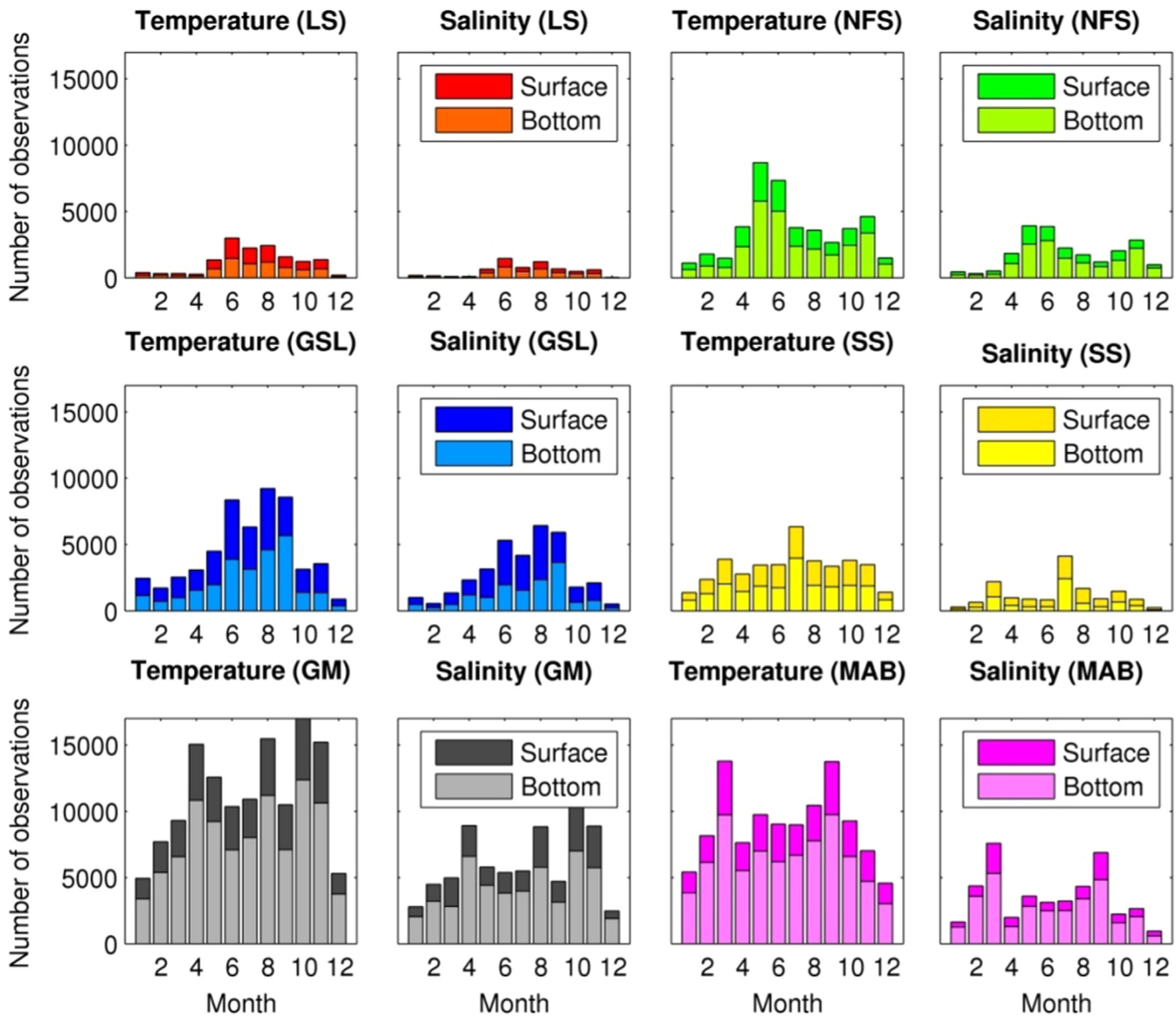

Fig. 4. Number of available observation for each month, region (shown in Fig. 2) and variable. The darker shade is for the surface. The y-scale is identical for all the pannels.

applied to the sea surface temperature (SST) and sea surface salinity (SSS). Also note that extrapolations are only performed between 1970 and 2010, when observations are relatively well distributed, thus ensuring both a more reliable interpolation and taking into account possible interannual variations. The Gulf of St. Lawrence was considered as a separate region in this exercise, because of its obvious hydrographic differences compared to similar latitudes to the east owing to strong fresh water influences. Finally, the sparser coverage of the Labrador Shelf did not support a robust enough seasonal cycle. For this reason, we processed SST only and exclusively in summer and fall (June to December) for this region.

The temporal coverage of the dataset is significantly improved by this gap-filling as demonstrated for the Gulf of St. Lawrence in Fig. 7. The differences in data coverage before (left in Fig. 7) and after (right in Fig. 7) processing for SST and SSS is clearly visible between 1970 and 2010, as the red and black dots replaced most of the yellow ones, nearly doubling the number of values and filling most data gaps. The resulting dataset should give a nearly equal weight to all months and years in the final averages for the climatology. Fig. 8 shows the data coverage after gap-filling for each region. As noted earlier, extrapolations on the Labrador Shelf were limited to SST from June to December. Finally, each variable is averaged for each grid and month to create the final monthly mean climatology at 0.2°x0.2° resolution for 1950–2010.

3. Seasonal climatology

Because of the wide extent of our study area, seasonal variations in surface and bottom temperature and salinity are likely to present a dependence on latitude and/or depth. Therefore, the mean seasonal cycles are separately calculated for each 3-degree latitude region from north to south. Each region is displaced southward by 3 degrees from the previous region, so that the adjacent regions do not overlap. Of course, three degrees in latitude is not always wide enough to have data all year round, especially in the northern most regions. We thus have some gaps

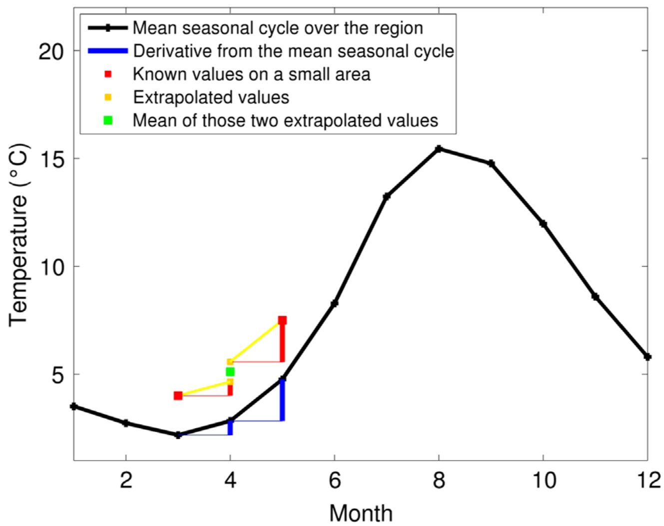

Fig. 5. Schematic diagram explaining the extrapolation method. The black curve represents the mean seasonal cycle constructed for a rather large area (5 degrees in latitude and 20 m of bathymetry) and a long time span (1970–2010). A missing value (green square) is extrapolated from the two known values in the bounding months (red squares) using the slope of the reference seasonal cycle (blue vertical lines). (For interpretation of the references to color in this figure legend, the reader is referred to the web version of this article.)

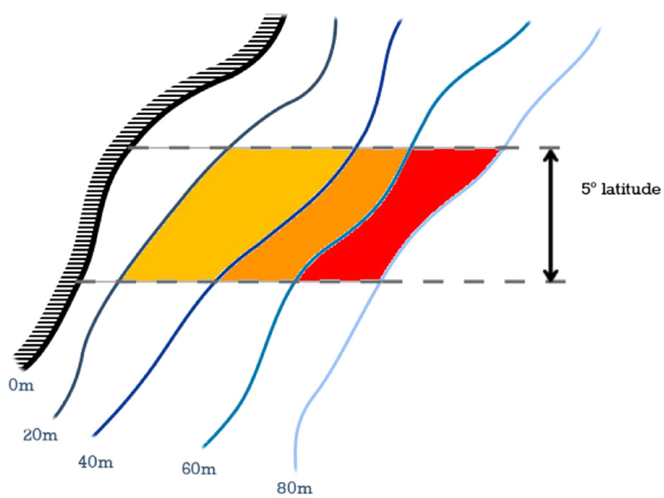

Fig. 6. Schematic illustration of the subregions spanning 5 degrees in latitude and a 20 m range in bathymetry used for calculating a mean seasonal cycle from monthly averages of data collected between 1970 and 2010 as detailed in Section 2.3. Each subregion is indicated with different color. (For interpretation of the references to color in this figure, the reader is referred to the web version of this article.)

in the seasonal cycles. Note that this sliding region is adapted to geographic constraints: the Gulf of St. Lawrence is considered separately for reasons that have already been discussed; the Laurentian Channel separates east and west regions, whose characteristics are different and the Newfoundland shelf is considered as one region, despite the fact that it is more than 3 degrees wide. Fig. 9 shows these regions, where colors for each region correspond to those used for the seasonal cycles in the following figures and we refer to the regions by the numbers written aside. In addition, the dependence on bottom depth is considered for some of the analysis by separately calculating the seasonal cycle on the shelf (0–200 m bottom depth) and upper slope (200–600 m bottom depth).

3.1. Surface seasonal cycles

The mean SST (Fig. 10, left panel) exhibits typical sinusoidal seasonal cycles, which are highly significant based on the standard errors. The minimum is always reached in March. The maximum is found in August for all 9 latitude bands. The SST range exceeds 7 °C on the northern Labrador Shelf (region 2 ; −1.5 to 5.9 °C) and increases southward to reach a maximum of ~16 °C (region 9; 7.2–23.8 °C) in the Mid-Atlantic Bight. With cold winter temperatures and rapid warming in spring, the SST range in the Gulf of St. Lawrence (region 6) exceeds 15 °C, which is ~3 °C larger than the adjacent Newfoundland (region 5) or Scotian Shelf (region 7). Our results are consistent with those from Drinkwater and Gilbert (2004) for the Gulf of St. Lawrence and the Scotian Shelf, and those from Shearman and Lentz (2010) in the Gulf of Maine and the Mid-Atlantic Bight. The standard error suggests slightly higher variability in summer for the regions 2–5.

The typical sinusoidal seasonal cycles suggest that the SST is mainly controlled by atmospheric conditions. In Fig. 11, the mean seasonal cycles of the net air-sea heat flux, averaged between 1984 and 2009 from the 1° × 1° OAFlux (Yu et al., 2008), are compared with the time derivative of SST, i.e. the differences between adjacent months progressively shifted by half of a month. To better compare the two curves, the derivative of temperature was multiplied by the heat capacity $Cp = 5000\ J\ °C^{-1}\ kg^{-1}$, the density $\rho_o = 1025\ kg\ m^{-3}$ and a characteristic depth scale $H_0 = 30$ m. The order of magnitude of the net air-sea heat flux agrees with the derivative of surface temperature, supporting the idea that this approximation is reliable. The two seasonal cycles share some common features and also some distinctions. The maxima are located in June-July for both parameters as clearly illustrated for the region 8 in bottom panel of Fig. 11. It is surprising that there is no significant latitudinal dependency in the amplitude or the timing of the maxima in either variable. On the other hand, the minima are reached between September and October for the time derivative of SST, while the heat flux minimum occurs between December and January. This discrepancy is likely due to the deepening of the mixed-layer and entrainment of colder water from below when the heat flux changes sign around September-October. Since the depth of the seasonal mixed-layer is not determined from our analysis, it is difficult to quantify the relative importance of advection and air-sea heat flux in the seasonal cycle of SST. However, the shape of the net heat flux implies that the air-sea heat flux plays a dominant role in setting the seasonal cycle of SST. This is consistent with the results obtained by Chen et al. (2014) for the Gulf of Maine and the Mid-Atlantic Bight. The SST is strongly correlated with the air temperature from the OAFlux, with a mean time correlation coefficient of 0.94 averaged over the whole region.

The seasonal cycle of SSS, while relatively more irregular and variable, has some interesting features (Fig. 10, right panel). The shelf and slope water are relatively fresh due to the influence of numerous rivers along the coast and the advection of subarctic water by the coastal boundary current (Loder et al., 1998 ; Fratantoni and McCartney, 2010). The amplitude of the seasonal cycle varies regionally, with the Labrador Shelf (region 2 ; 31.2–33.7 psu) and Mid-Atlantic Bight (region 9 ; 31.1–33.4 psu) exhibiting larger amplitudes relative to the Scotian Shelf and Gulf of Maine. This could be explained by the sea-ice coverage of the Labrador Shelf in winter (Fig. 1), reducing 2–3 m of freshwater in the water column (Khatiwala et al., 1999) and the influence of salty Slope Water in the Mid-Atlantic Bight. The Gulf of St. Lawrence is much fresher compared to the rest of the regions with the surface salinity dropping to 29.2 psu in June-September and reaching only 31.5 psu in January-April. April-May corresponds to the maximum discharge of the St. Lawrence river (Bourgault and Koutitonsky,

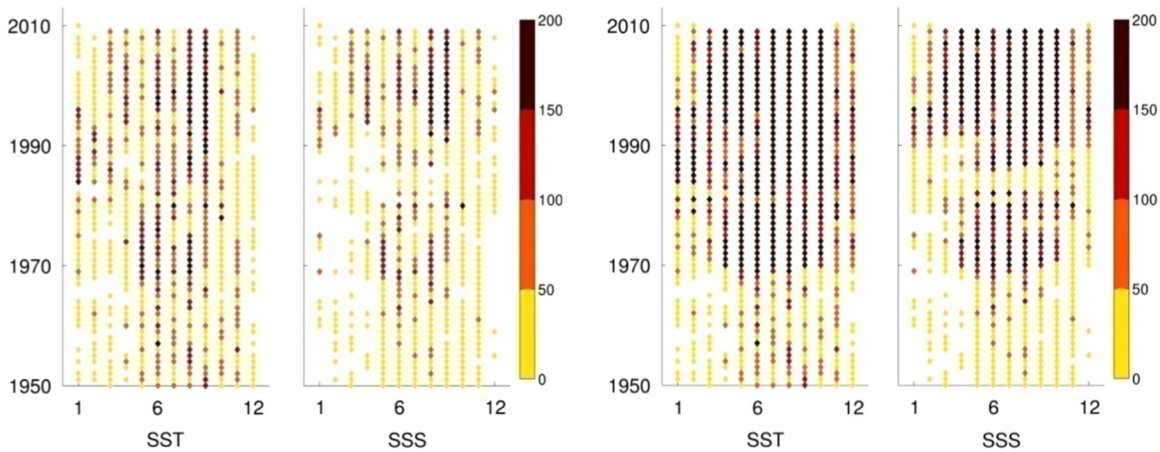

Fig. 7. Data coverage before (left) and after (right) the gap filling process, in the Gulf of St. Lawrence. The color of each dot represents the number of available data for each month (X axis) of each year (Y axis). (For interpretation of the references to color in this figure, the reader is referred to the web version of this article.)

1999), consistent with the seasonal decrease in the regional average climatology. For all the other regions, minima are reached in July or August and maxima in January or February, with the annual means staying around 32 psu without a clear latitudinal dependency. Indeed, there is no significant correlation between surface salinity and latitude.

3.2. Bottom seasonal cycles

Fig. 12 shows seasonal cycles for the bottom temperature and salinity. Because these signals may be sensitive to the bottom depth, a distinction is made between shelf, ranging from 0 to 200 m (left panels), and slope from 200 to 600 m (right panels). Since the shelf break is situated around 50 m in the Mid-Atlantic Bight and at 400 m over the Labrador Shelf, this shelf-slope distinction is only a rough estimate. However, using a more exact local shelf break definition does not significantly change the results presented below. It should be noted that this bathymetric definition does not simply imply that “shelf” refers to any observation inshore of the shelfbreak and “slope” refers to any observations offshore of the shelfbreak. By this definition, regions on the continental shelf that are deeper than 200 m, such as the deep basins and channels in the Gulf of Maine and on the Scotian Shelf, are considered part of the slope region.

Bottom temperature has a well-defined seasonal cycle over the shelf, at least in the four southern regions (regions 6–9), reaching a minimum in March as in SST and maximum in October-November, lagging SST by 2–3 months (as shown for region 8 in the bottom panel of Fig. 11). The amplitude ranges between 4.0 and 6.5 °C in the three southern most regions, i.e. the Scotian Shelf, Gulf of Maine, and Mid-Atlantic Bight. From the Gulf of St. Lawrence to the Labrador Shelf, the seasonal amplitude is substantially reduced, barely exceeding 2 °C. The Labrador Shelf (region 2–3), protected by sea-ice for an extended period of time, seems even slightly warmer in winter (1.1 °C in December) than in summer (-0.5 °C in August), though the difference is hardly statistically robust due to the small number of observations in the region, as shown by the standard errors, especially in winter. Also note that only a limited area of the Labrador Shelf is shallower than 200 m (Fig. 9). The weak seasonality observed at the bottom in the northern regions may be explained by the bathymetry, since the Labrador Shelf is 150 m deep on average and thus less influenced by surface forcing. In fact, the correlation between the amplitude of the seasonal cycle and the depth is -0.74. In the Gulf of St. Lawrence and on the Scotian Shelf, the Cold-Intermediate Layer insulates the bottom water in summer (Drinkwater and Gilbert, 2004), resulting in a weak seasonal cycle in the bottom temperature. The annual mean bottom temperature changes much more abruptly from north to south compared to the more gradual change observed in SST. The mean bottom temperatures in the Gulf of St. Lawrence and regions to the north (regions 1–6) range between 0.5 and 2.6 °C, while mean bottom temperatures are distinctly warmer in the three southern regions (regions 7–9), measuring 6.3–10.4 °C.

Without surprise, considering its depth and lack of direct interaction with the atmosphere, there is no discernible seasonal cycle in bottom temperature over the slope (Fig. 12). The annual range is between 0.6 and 2 °C for all 9 regions, with a standard deviation of roughly the same order, ranging between 0.8 °C for the Labrador Shelf and 1.8 °C for the Mid-Atlantic Bight. However, there is a clear latitudinal dependency to the bottom temperature. Similar to the shelf, the annual mean temperatures on the slope are similar for the northern five regions (Labrador to Newfoundland), averaging roughly 2.3 °C. By comparison, the annual mean bottom temperature in the Gulf of St. Lawrence is 4.8 °C, this water being mainly Slope Water concentrated at depth in the Laurentian Channel. Finally, there is a large jump to $\sim$8 °C in the deep basins of the Gulf of Maine and Scotian Shelf, and to $\sim$10.6 °C in the Mid-Atlantic Bight. The latitudinal dependence of bottom temperatures revealed by the climatology reflects the shift in the composition of the Slope Water masses, from a dominance of subpolar sources in the north to subtropical sources in the south (Gatien, 1976; Mountain, 2012).

Bottom salinity is the noisiest and thus the most difficult to interpret among all four variables (Fig. 12). The clearest signal is that the Slope Waters are significantly saltier than shelf waters, by roughly 1.5 psu. The bottom salinity in the Gulf of St. Lawrence on the shelf is about 1 psu fresher than the rest of the regions, while the very strong seasonal cycle of surface salinity in the Gulf of St. Lawrence is barely visible at the bottom, a consequence of the strong stratification associated with fresh river discharge. On the upper slope, the southern regions are generally saltier due to the proximity to the Gulf Stream. In particular, the Mid-Atlantic Bight (region 9) is about 1 psu saltier than the rest of the regions.

3.3. Meridional phase lags

The normalized seasonal cycles of SST and SSS are plotted for

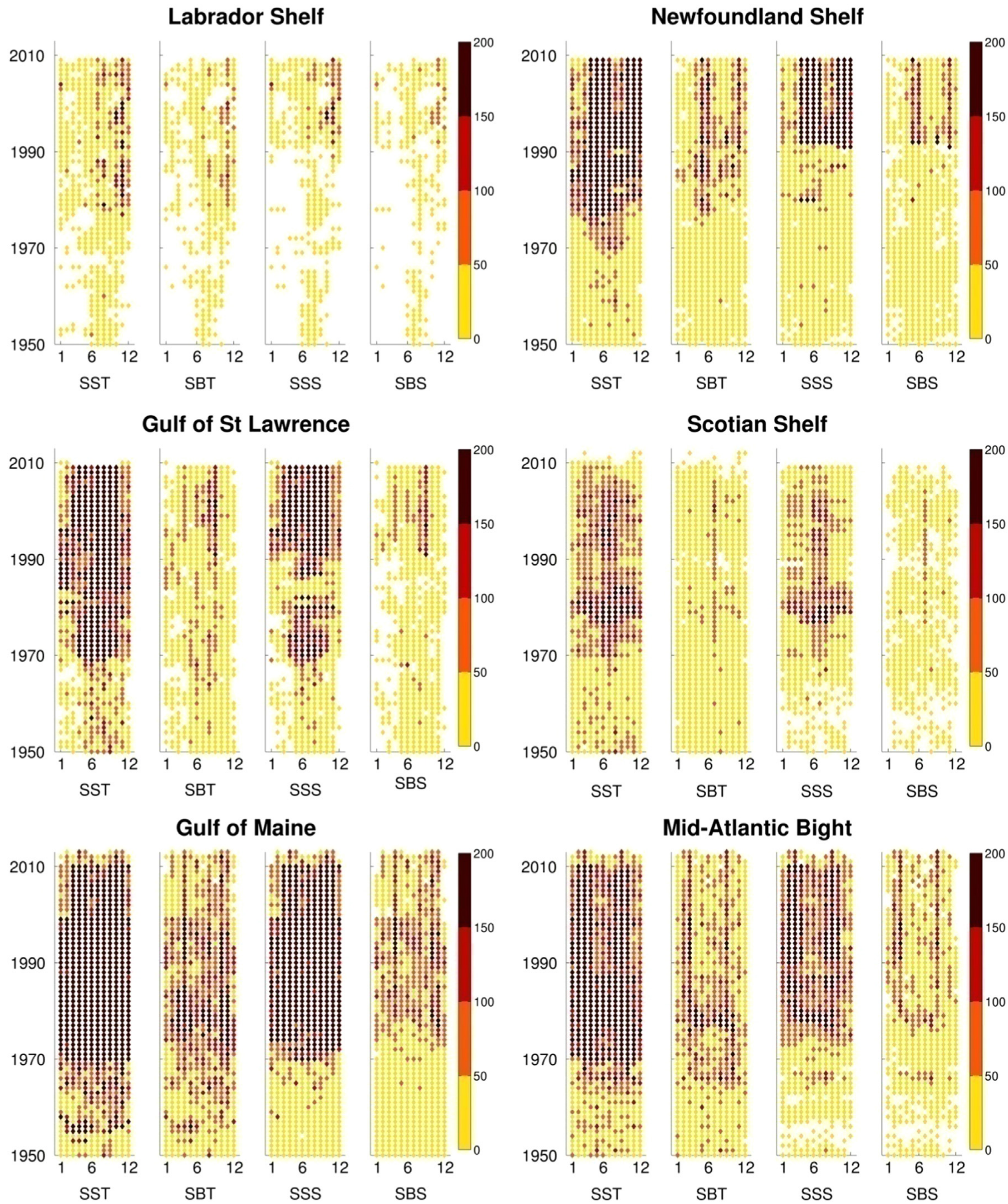

Fig. 8. Temporal distribution of available data, for all six regions, after extrapolation. Gap-filling was only applied to surface temperature between June and December on the Labrador Shelf, while surface temperature and salinity were filled year-round in all other regions. Colors indicate the number of stations. SST, SBT, SSS and SBS stand for sea-surface temperature, sea-bottom temperature, sea-surface salinity and sea-bottom salinity, respectively. (For interpretation of the references to color in this figure, the reader is referred to the web version of this article.)

the 9 meridionally-oriented regions to examine any meridional phase propagation of the seasonal cycle (Fig. 13). The normalized seasonal cycle is defined as $2 \times (X - X_{min})/(X_{max} - X_{min}) - 1$, where the X is the climatological monthly values of SST or SSS, and (X_{max}-X_{min}) is the amplitude of the seasonal cycle. The northern Labrador Shelf (region 1) is excluded from this calculation as the full seasonal cycle is not resolved by the climatology.

The SST clearly exhibits a meridionally coherent seasonal cycle without any phase lag (left panel of Fig. 13). However, SSS exhibits more interesting features: the minima of the four northern boxes, extending from the Labrador Shelf to the Newfoundland Shelf, appear to be propagating southward in agreement with the mean direction of the circulation. The distance from the northern Labrador Shelf to the Tail of the Grand Banks is approximately 2000 km, hence the lag between those two places (around 4 months) would give roughly 20 cm/s for the propagation speed, consistent with the magnitude of the current velocity over the Labrador Shelf (Fratantoni and Pickart, 2007; Fratantoni and

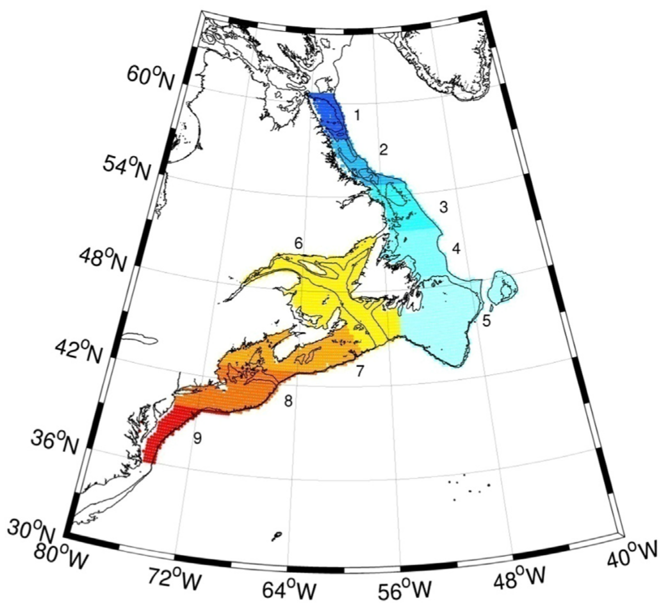

Fig. 9. Each color shows the 3-degree regional definitions. All regions measure roughly 3-degree wide, except for the GSL, which is considered separately. Contours show the coast and the 200 m and 600 m isobaths. The colors are carried through to indicate region in the following plots. (For interpretation of the references to color in this figure, the reader is referred to the web version of this article.)

McCartney, 2010). South of the Newfoundland Shelf, there is no indication of propagation, all maxima and minima occur in the same month. This could mean that the river discharges, all occurring at the same time along the shelf, dominate the phasing of the seasonal cycle south of the Laurentian Channel.

4. Seasonal maps

4.1. General maps

A complementary view of the seasonal cycle and its propagation along the North American east coast can be given by mapping the seasonal distribution of temperature and salinity. The four seasons are defined according to the above-described seasonal cycles: spring is from April to June, summer from July to September, fall from October to December, and winter from January to March. The gridded temperature and salinity are averaged over all months and all years. Whenever one or more of the months was missing, the average was made with the remaining ones. This is not a problem for summer and winter, when temperature and salinity are relatively stable, but can introduce biases for the two other seasons, when large seasonal changes are occurring. The seasonal mean SST, SSS, bottom temperature and bottom salinity are shown in Figs. 14–17, respectively. While previously described features are also evident here, some notable new features emerge.

The most noticeable pattern in SST is a clear latitudinal dependence. Spatial correlations between SST and latitude range between −0.83 in winter and −0.92 in fall. In winter, only the Mid-Atlantic Bight is warmer than 5 °C, while in summer the temperature is above 10 °C everywhere except on the Labrador Shelf.

In contrast, the SSS appears more correlated with bottom depth than latitude. Spatial correlations between SSS and bottom depth range from 0.19 in summer to 0.23 in fall. Near-shore waters are fresher than offshore ones, due to freshwater discharge. The influence of St. Lawrence river runoff is the most striking, evident as a plume of freshwater (less than 30.5 psu) primarily concentrated in the southwestern half of the Gulf of St. Lawrence (due to geostrophy), exiting the Gulf through the Laurentian Channel and expanding both westward along the coast and southward across the Scotian Shelf. Signatures of freshwater sources are also evident in the Gulf of Maine near the St. John river, and in the Mid-Atlantic Bight, especially near the Chesapeake Bay. While this near-shore freshening is visible during all seasons, it is most striking in summer, even though the maximum discharge for all rivers occurs in spring. On the other hand, the highest surface salinity is reached offshore of the Mid-Atlantic Bight, north of Cape Hatteras and over Flemish Cap, reflecting the influence of the Gulf Stream and Slope Water.

Bottom temperature and salinity underline the bathymetry of the region, with relatively warm and salty water observed in the Laurentian Channel and the Northeast Channel (north of Georges Bank), but also in the deep basins of the Gulf of Maine and the Emerald Basin on the Scotian Shelf. This is a signature of Slope Water entering the domain (Mountain and Manning, 1994). Yet, while the spatial correlation of bottom salinity with bathymetry varies between 0.49 in spring and fall and 0.57 in summer, the correlation between bottom temperature and bathymetry is only –0.32 in fall, dropping to 0.0 in winter and spring. This is because the bottom temperature is still mainly governed by latitude, whose correlation is as high as −0.74 in fall. As pointed out in the previous section, seasonal variations in bottom temperature are barely visible east and north of the Laurentian Channel. In the Mid-Atlantic Bight, the shallow areas exhibit larger seasonal

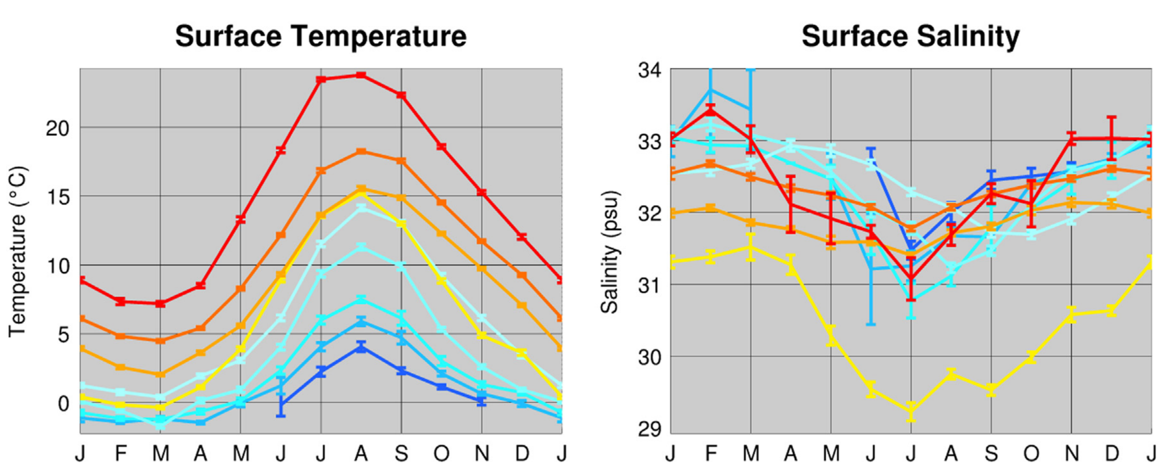

Fig. 10. Seasonal cycles of sea surface temperature (SST) (left) and salinity (right). Colors correspond to the regional definitions in Fig. 9. January is plotted twice, for continuity. The average includes 1950–2013. The vertical bars indicate the standard error of each monthly mean value.

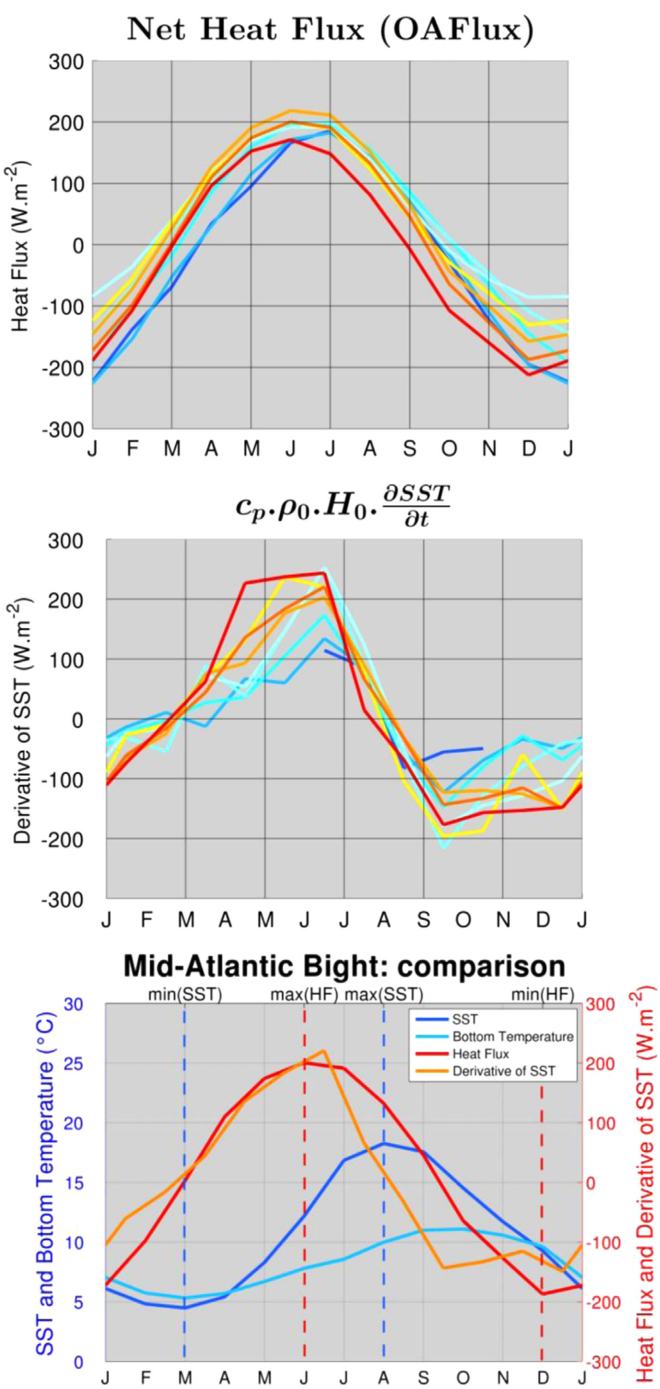

Fig. 11. Net air-sea heat flux from atmosphere to ocean where positive indicates heat gain by the ocean (top) and derivative of the SST (middle). Colors correspond to the regions defined in Fig. 9. The net heat flux is from the OAFlux (Yu et al., 2008). (Bottom) Comparison between the net air-sea heat flux (red), derivative of SST (orange), SST (blue), and bottom temperature (light blue) for the region 8. (For interpretation of the references to color in this figure legend, the reader is referred to the web version of this article.)

variations, with temperatures lower in winter and warmer in summer. Seasonal variation is very small for bottom salinity.

4.2. Stratification

As our climatology does not include vertical profiles of temperature and salinity, we infer the vertical stratification from the surface minus the bottom values of density (Fig. 18). Our measure will practically reflect whether the mixed-layer reaches the bottom. Localized studies, such as Li et al. (2015), give a more exhaustive description of the stratification. To further quantify the respective contributions of salinity and temperature to the stratification, we also present the density ratio based on thermal expansion and haline contraction coefficients (Fig. 19).

Overall, strong stratification (< -1.25 kg m^{-3}) dominates over most of the area year-round. Yet, there are a few regions where the inferred stratification is particularly small, such as Georges Bank and in portions of the Bay of Fundy, where the density difference is smaller than -0.5 kg m^{-3}. Energetic tidally-driven vertical mixing maintains relatively homogenous conditions year round (Garrett and Loder, 1981). Some other seasonal homogenizations are taking place over the Mid-Atlantic Bight in fall and winter and over the Grand Banks in winter and spring. Stratification is much stronger in summer (even compared to spring) consistent with regional studies such as Li et al. (2015). The turbulent tidal process occurring on the shallow Grand Banks mixes approximately the deeper 50% of the water column (Han, 2000). But cold, winter temperatures probably initiate convection to mix waters from surface to bottom, with additional tidal mixing. Overall, the density difference exhibits strong negative correlation with the bottom depth with maximum in winter ($r = -0.79$) and minimum in spring ($r = -0.55$).

Fig. 19 also gives interesting information about the relative role of salinity and temperature in the density stratification, through the calculation of the density ratio:

$$\gamma = -\frac{\alpha \times (SurfaceTemperature - BottomTemperature)}{\beta \times (SurfaceSalinity - BottomSalinity)}$$

where α is the thermal expansion coefficient ($= -\frac{1}{\rho}\frac{\partial \rho}{\partial T}$) and β is the saline contraction coefficient ($= \frac{1}{\rho}\frac{\partial \rho}{\partial S}$). Since salinity is always lower at the surface than the bottom (Figs. 15 and 17), negative values correspond to a negative contribution of temperature (i.e. surface temperature < bottom temperature). Furthermore, as the water column is always stably stratified (Fig. 18), i.e. $\Upsilon > -1$, salinity gradient is responsible for making the water column stable when Υ is negative. This is the case over most of the area in winter. When the ratio is positive but smaller than one, the contribution of salinity is greater, while temperature contribution is more important if the ratio is greater than one. According to Fig. 19, salinity has a greater influence on stratification for most of the year (ratio often less than 0.5), except over the Mid-Atlantic Bight and the Grand Banks between spring and fall, where the ratio is greater than 2. Shallow regions such as Sable Island Bank and the western part of the Gulf of Maine also exhibit a greater contribution of temperature in summer, which is consistent with the results obtained by Li et al. (2015).

5. Summary and discussion

5.1. Summary

A seasonal hydrographic climatology is presented for the continental shelf region extending from the northern tip of the Labrador Shelf to Cape Hatteras. The climatology combines surface and bottom temperature observations from Canadian and U.S. archives and offers an opportunity to examine spatial patterns in seasonal variability across the region as a whole.

The mean seasonal cycle of surface temperature is primarily controlled by the surface heat flux, while its spatial distribution is highly correlated with latitude. The net heat flux also seems to be the primary driver of the mean seasonal cycle of the bottom temperature on the shallow shelf regions south of the Laurentian Channel, where seasonal cycles have a relatively large amplitude

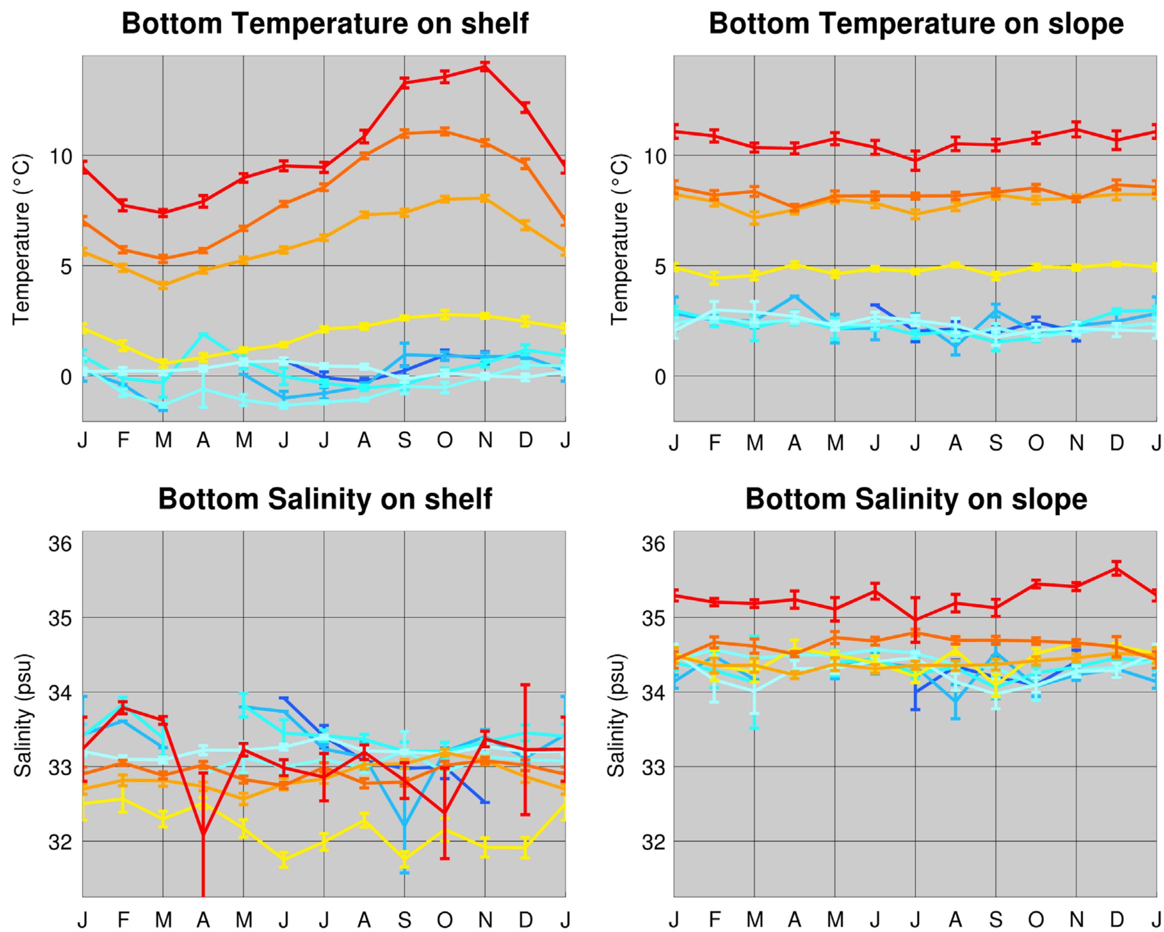

Fig. 12. Mean seasonal cycles of bottom temperature (top panels) and salinity (bottom panels) on the shelf (left) and slope (right). Colors correspond to the regions defined in Fig. 9. The vertical bars indicate the standard error of each monthly mean value. (For interpretation of the references to color in this figure legend, the reader is referred to the web version of this article.).

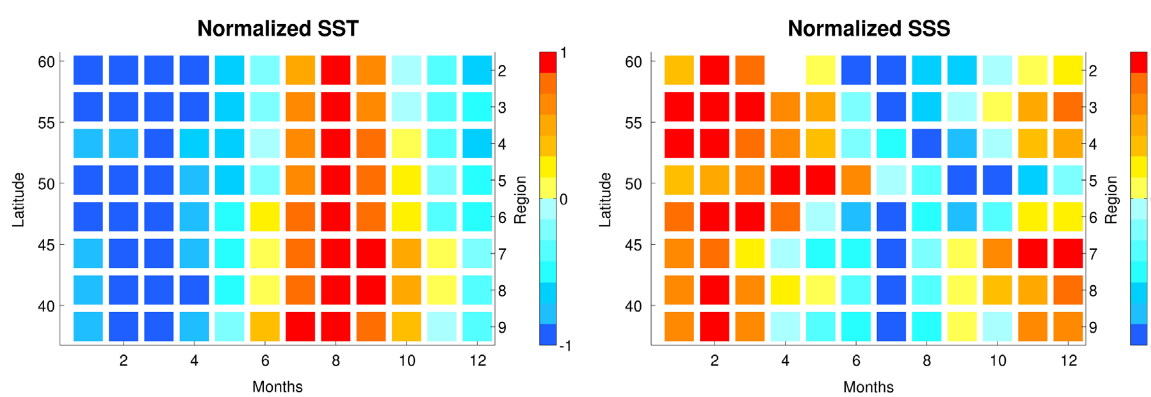

Fig. 13. Normalized mean seasonal cycles for SST (left), and SSS (right). Each row corresponds to one of the regions depicted in Fig. 9, with corresponding numbers shown to the right. Each mean seasonal cycle is normalized so that the maximum and minimum values correspond to 1 and −1, respectively.

compared to the region to the north. The influence of evaporation minus precipitation on the surface salinity was not assessed in this paper. However, the influence of river discharge is clear in the surface salinity, especially in the Gulf of St. Lawrence and regions to the south. On the other hand, sea ice appears to be another important element for the surface salinity variability in the regions to the north (Deser et al., 2002; Khatiwala et al., 1999). The bottom salinity distribution is strongly constrained by bathymetry. The intrusions of salty Slope Water over the shelf through the deep channels and the strong vertical mixing in the tidally energetic regions leads to the mixing of different water masses.

5.2. Meridional coherence

The coherence of seasonal mean water mass properties is best summarized by the evolution of the regional temperature-salinity

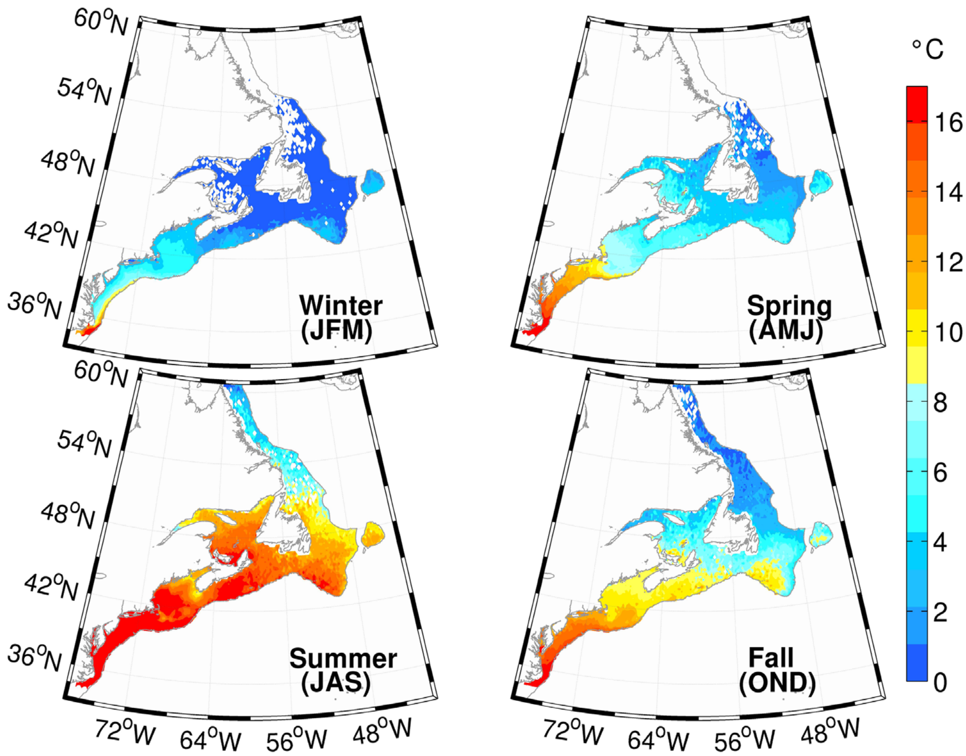

Fig. 14. Mean (1950–2013) seasonal maps of SST. The scale is the same all the four maps. The 600 m isobath is indicated by the gray contour.

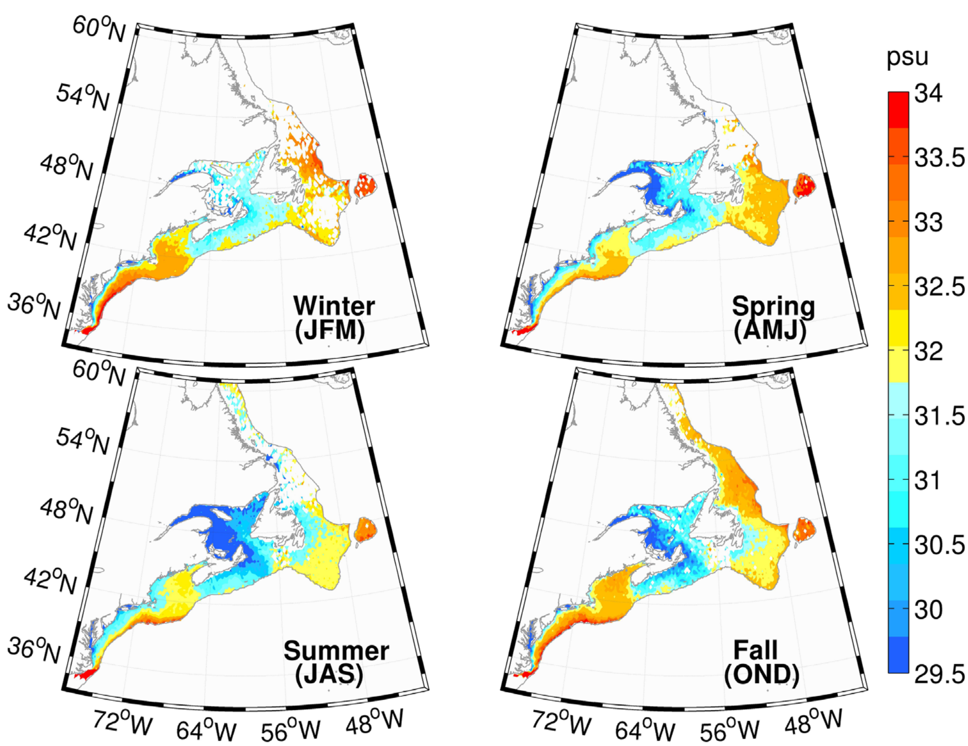

Fig. 15. Mean seasonal maps of SSS. The 600 m isobath is indicated with the gray contour.

relationship, progressing from north to south (Fig. 20). On the slope, where the water depth exceeds 200 m, summer bottom temperature and salinity is distinctly clustered in northern (0–4 °C, 34–35 psu) and southern regions (7–12 °C, 34.5–35.5 psu), with a clear separation at the Gulf of St. Laurence. On the shelf, the temperature varies primarily in the north-south direction while salinity varies in the cross-shelf direction. This is true for all four seasons at both surface and bottom. Again, the Gulf of St. Laurence represents a boundary between the northern and southern regions, with more or less homogenous conditions to the north and a range of rapidly warming temperatures to the south, consistent with the surface temperature distribution in winter (Fig. 10).

Furthermore, the occurrence of the seasonal minima in surface salinity on the Labrador and Newfoundland Shelves shows a clear

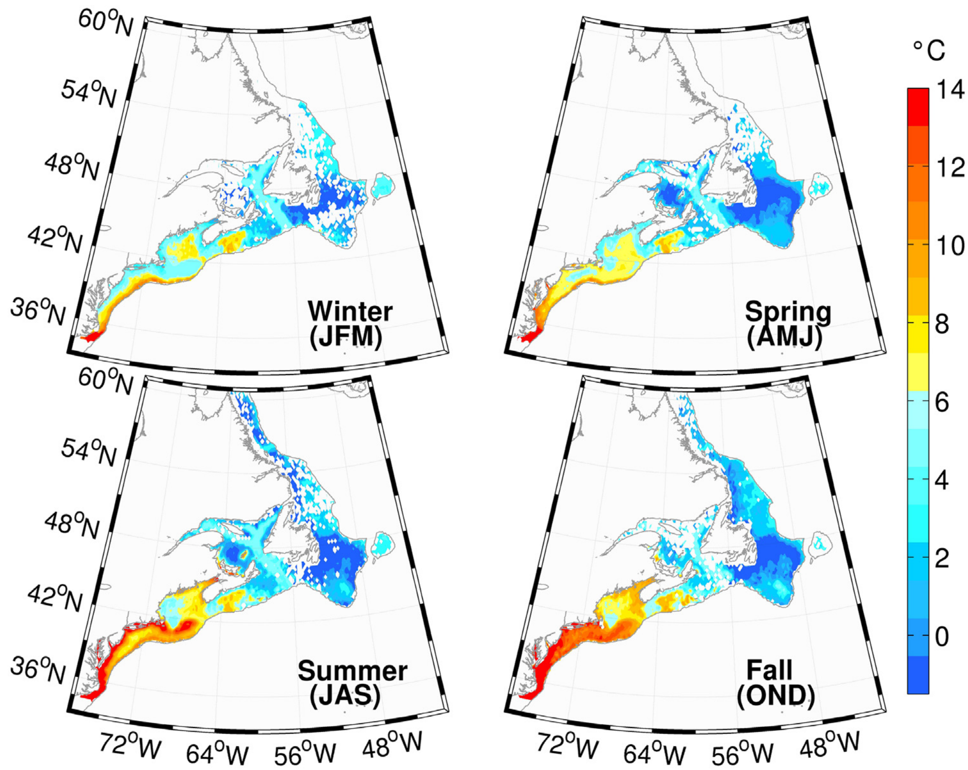

Fig. 16. Mean seasonal maps of bottom temperature. The 600 m isobath is indicated with the gray contour.

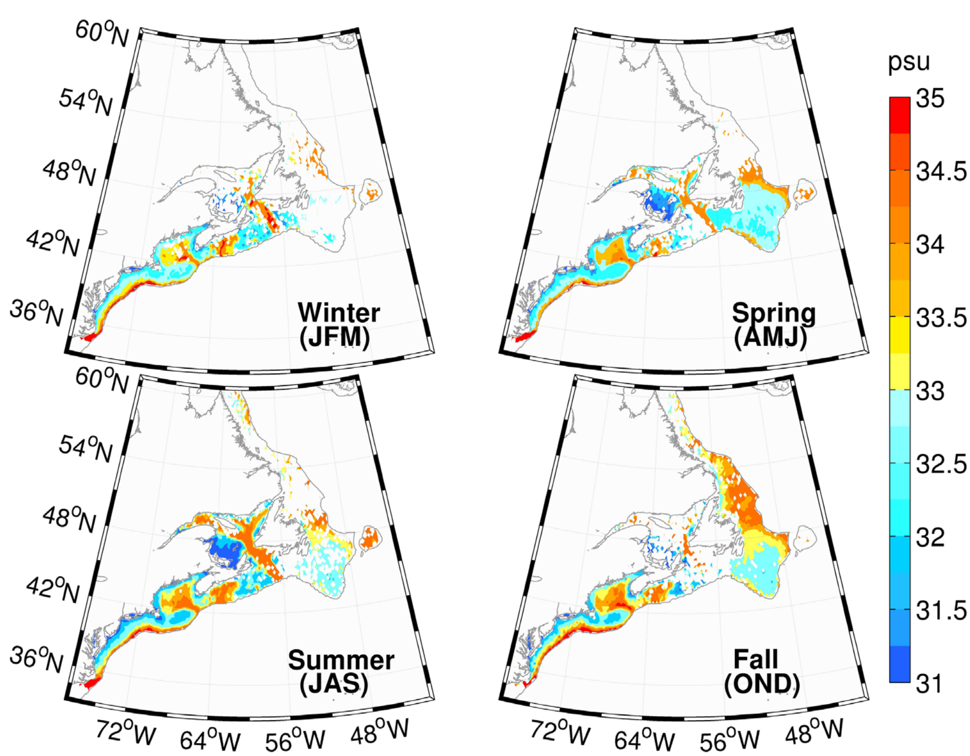

Fig. 17. Mean seasonal maps of bottom salinity. The 600 m isobath is indicated with the gray contour.

phase lag from north to south, with a phase speed that is consistent with observations of mean southward current speeds in the region. However, the Laurentian Channel disrupts this pattern of southward propagation, marking the division between the northern and southern regimes. The absence of a propagating signal in SST, SSS, and bottom temperature on the shelf in the southern region likely indicates that local forcing dominates in these relatively shallow regions, even though the mean circulation is still southward. The meridional phasing of the seasonal cycle along the Canadian shelf and upper slope especially for the surface salinity has barely been suggested in previous literature. Fratantoni and McCartney (2010) showed similar phasing in the Shelf

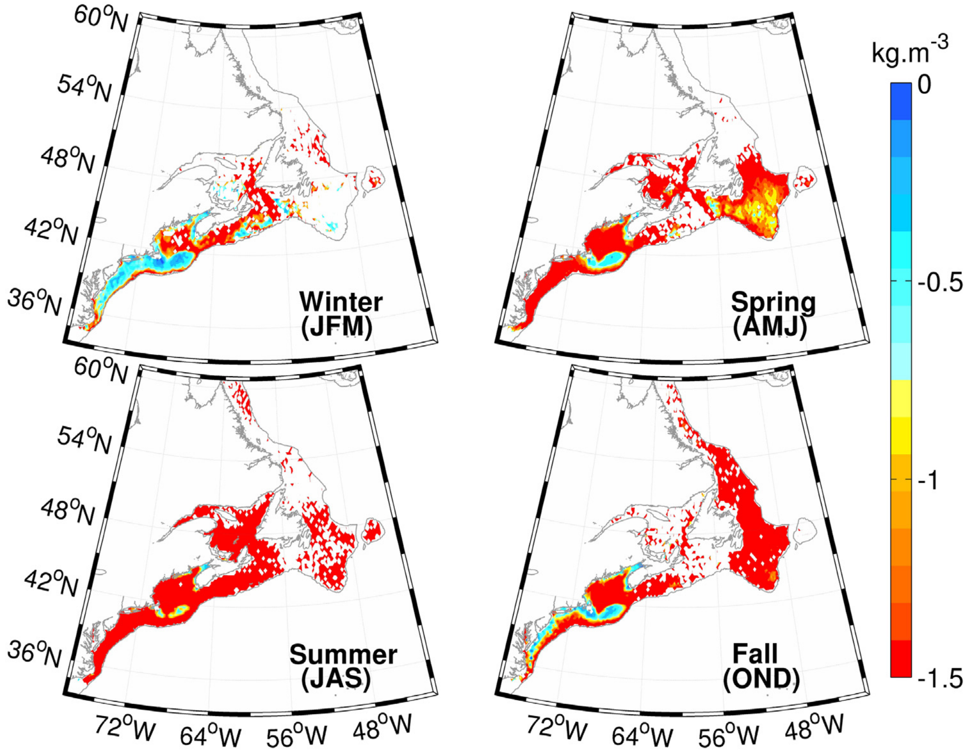

Fig. 18. Difference between surface and bottom density (surface minus bottom), for each season. The 600 m isobath is indicated with the gray contour.

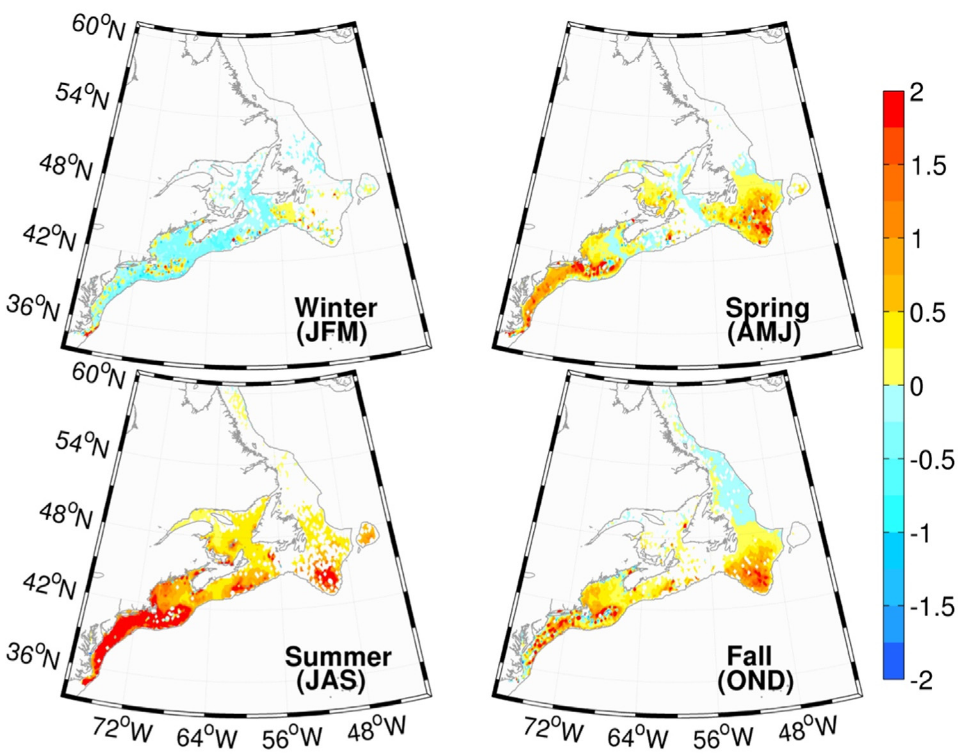

Fig. 19. Ratio for relative contribution to surface–bottom density difference, temperature contribution over salinity contribution as defined in the text. Values between –1 and +1 indicate dominance of salinity, while values greater than 1 indicate dominance of temperature. Because surface salinity is always lower than bottom here, negative values only occur when surface temperature is smaller than the bottom temperature, with salinity differences providing water column stability. The 600 m isobath is indicated with the gray contour.

Water Layer ($\sigma_0 \leq 26.80$), estimating a 3 month lag between the timing of minimum salinity on the Labrador Shelf and at the Tail of the Grand Banks of Newfoundland.

On the other hand, the equatorward propagation of bottom temperature anomalies on interannual to longer time scales was previously reported in several studies along the upper slope (Frankignoul et al., 2001; Peña-Molino and Joyce, 2008) and shelf (Rossby and Benway, 2000; Shearman and Lentz, 2010) for various

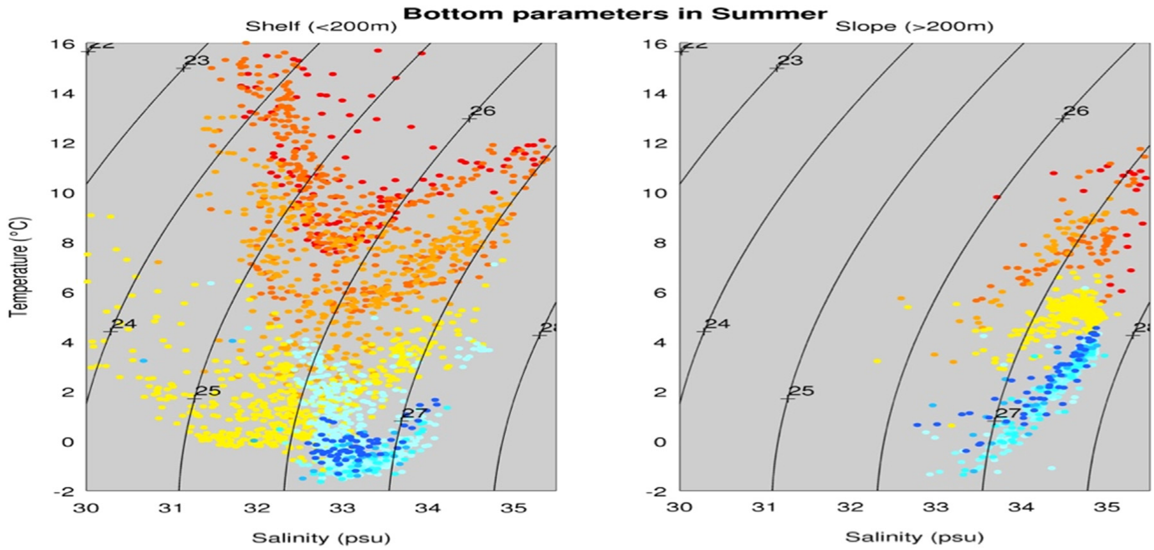

Fig. 20. Temperature-salinity diagram for the bottom values on the shelf (left) and slope (right) in summer. Colors correspond to the regions defined in Fig. 9. (For interpretation of the references to color in this figure legend, the reader is referred to the web version of this article.).

parts of the shelf and slope. In addition, Xu et al. (2015) recently suggested that the interannual SST anomalies associated with the North Atlantic Oscillation propagates from the Labrador Sea to the Gulf of Maine along the shelf and upper slope. A preliminary analysis based on our dataset suggests that the interannual variability of SST and bottom temperature anomalies along the shelf and upper slope are highly correlated. Work is still needed to better understand the mechanisms controlling meridional propagation of temperature and salinity anomalies on various time scales.

5.3. *Some regional aspects*

Our results focused on describing the meridionally coherent structure of the mean seasonal cycle of temperature and salinity over the entire domain. However, our new dataset has high enough spatial resolution to reveal the details of regional features. While regional studies using this dataset are beyond the scope of this paper, here we discuss further two sub-regions, as examples.

5.3.1. *Influence of St. Lawrence River*

A striking feature, especially visible in the surface maps, is the outflow of very fresh water from the St. Lawrence River (Fig. 15). The advection of fresh water is visible from the Gulf of St. Lawrence through Cabot Strait, and along the coastline toward the Scotian Shelf and the Gulf of Maine. Fig. 21 is an enlargement of the Gulf of St. Lawrence and the Scotian Shelf, showing the distribution of surface and bottom salinity during summer. The maximum freshwater discharge from the St. Lawrence River occurs in April (Bourgault and Koutitonsky, 1999). At a speed of 0.1 m/s (Wu et al., 2012) it would take approximately 3 months for discharge to reach Cabot Strait, along the 800 km distance from the lower St. Lawrence estuary. This is consistent with the timing observed in our climatology, where by summer, freshening is observed over the entire Gulf of St. Lawrence and over the Scotian Shelf. The development of the fresh plume is clearly visible on monthly maps (not shown here). This is corroborated by Fig. 22, representing the probability distribution of SSS and bottom salinity in spring and summer for the Gulf of St. Lawrence (as defined in Fig. 2). For SSS, the peak is visible at 31.5 psu in spring and at 30.5 in summer. In addition, the summer SSS distribution is skewed toward fresher values, suggestive of enhanced river runoff.

The strong along-channel front of SSS in the mouth of the Gulf

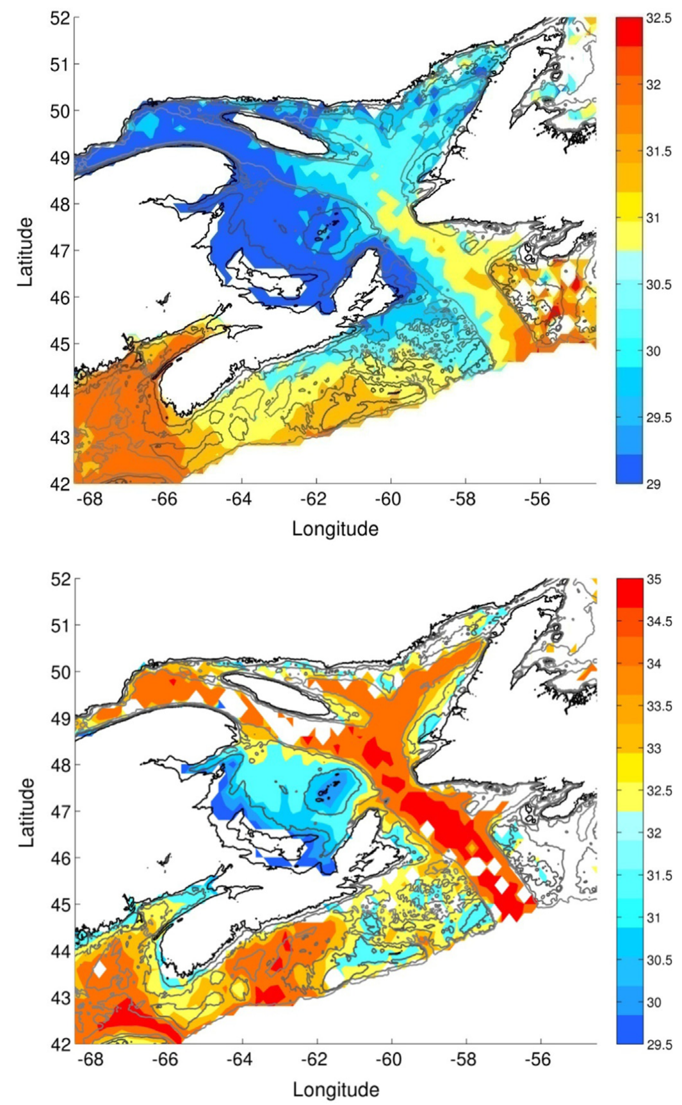

Fig. 21. Surface (upper panel) and bottom (lower panel) salinity distributions for the Gulf of St. Lawrence and the Scotian Shelf during summer (July-September). Contours indicate the 50, 100 and 200 m isobaths.

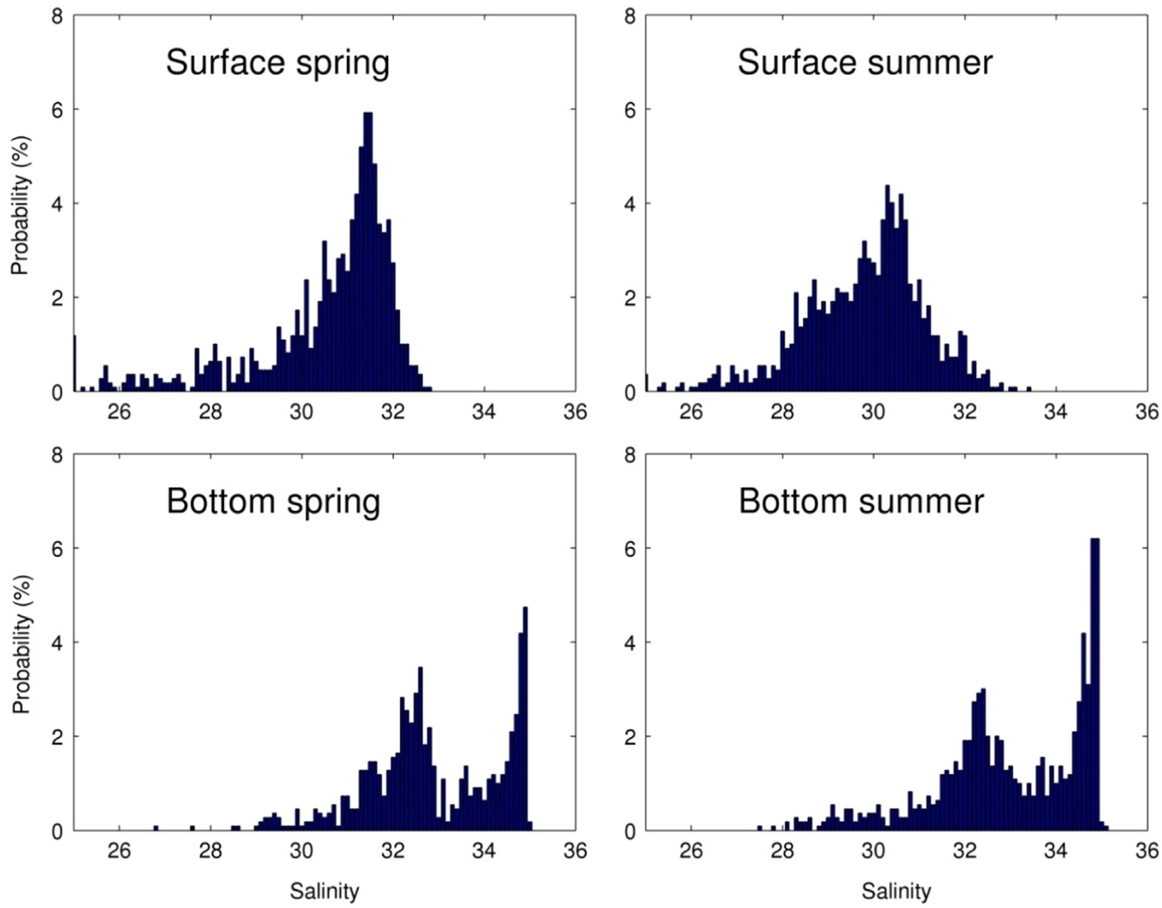

Fig. 22. Probability distribution of surface (top pannels) and bottom (bottom pannels) salinity in the Gulf of St. Lawrence during spring (left panels) and summer (right panels).

of St. Lawrence, which is more or less collocated with the 200m isobath, is clearly visible in Fig. 21. The salinity rises from less than 29 psu in the southwest to more than 31 psu in the northeast within ~50 km across Cabot Strait, which is 110 km wide. Lateral mixing is likely to occur along this front, even though we cannot confirm this in the climatology. We can see that relatively salty surface water flowing south from Newfoundland does not cross this front in the map. The mean circulation given by Fratantoni and Pickart (2007) in summer in this region indicates that there is an offshore westward current carrying this salty water over the slope instead of the shelf. The fresh plume flowing out of the Gulf of St. Lawrence is a curiosity, in that it follows the Laurentian Channel offshore to the edge of the Scotian Shelf, despite the fact that the mean circulation is southwestward. A branch of the plume does turn westward to follow the coast of Nova Scotia. It seems to be constrained near the shore less than 150 m deep by saltier water coming from the Newfoundland Shelf.

The bottom salinity map shows clearly salty Slope Water entering the Gulf through the deep Laurentian Channel, extending far into the estuary. The water entering the Gulf of St. Lawrence circulates cyclonically, mixing with surface waters near the estuary and over Magdalen Shallows and exiting in the southwestern part of Cabot Strait (Drinkwater and Gilbert, 2004). As it circulates around the Gulf, it freshens and cools, and will thus influence the downstream water properties of the Scotian Shelf, the Gulf of Maine and the Mid-Atlantic Bight. In Fig. 22, the bottom salinity exhibits two clear peaks, in spring as well as in summer. The primary peak, which is very steep and centered at 34.9 psu, indicates the presence of Slope Water. The secondary peak is situated at 32.6 psu in spring (32.4 in summer) and corresponds to the outflow influence by the river discharge. Both peaks are also present in winter and fall (not shown here).

5.3.2. *Role of bathymetry in Gulf of Maine*

A closer examination of the distribution of the water masses in the Gulf of Maine, in summer, clearly reveals the role of bathymetry (Fig. 23). The most noticeable feature is probably the bottom salinity dependence on the topographic features, with the saltier water in the Northeast Channel and the fresher water near the shore and over Georges Bank.

The Penobscot River on the northern coast of the Gulf of Maine and the St. John River in the Bay of Fundy are two important sources of fresh water whose influence is evident in maps of surface and bottom salinity. The fresh water input from the rivers spreads cyclonically along the boundary. Yet their maximum discharge occurs in spring rather than summer and their influence on salinity is more clearly seen in summer.

Mountain (2012) discusses three dominant water masses that enter the Gulf of Maine. Scotian Shelf Water (SSW) is the coldest and freshest source, having characteristic temperature and salinity values of 2 °C and 32.0 and entering the mid- to upper-layers of the Gulf of Maine from the Scotian Shelf. In addition, warmer/saltier Slope Water enters the Gulf of Maine at depth through the Northeast Channel, progressively spilling into the deep basins of the Gulf of Maine. The Slope Water consists of a mixture of Warm Slope Water (WSW ; 12 °C and 35.4 psu) derived from subtropical sources and Labrador Slope Water (6 °C and 34.6 psu) derived from subpolar sources. In the upper layers of the Gulf of Maine, shelf waters circulate counter-clockwise around the basin and are progressively modified by atmospheric fluxes of heat and

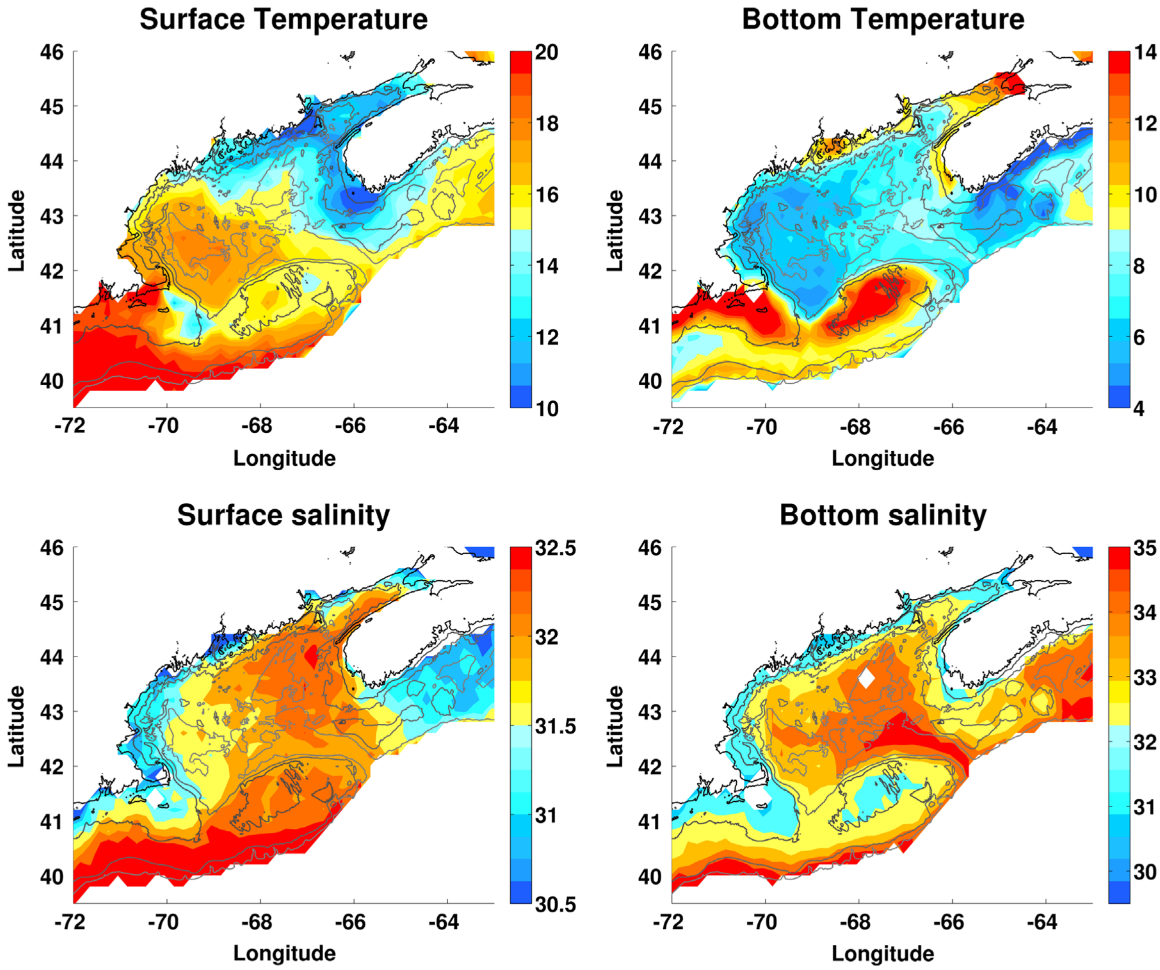

Fig. 23. Summer (July-September) temperature (top panels) and salinity (bottom panels) at surface (left) and bottom (right) in the Gulf of Maine. Contours indicate the 50, 100 and 200 m isobaths.

freshwater and through mixing with both deeper slope waters and the discharge of local rivers. The influence of the cold/fresh SSW is clearly visible in the climatological surface property maps (Fig. 23), spreading into the Gulf of Maine along the eastern boundary. This is distinguishable from the more saline Slope Water mixture entering at depth through Northeast Channel, and seems to be another significant source of freshwater. The two types of Slope Waters are not distinct in our climatology because they mix over the slope, before entering the Gulf, and their relative contribution varies according to years. However, the salty Slope Water entering the Northeast Channel is clearly seen in the bottom salinity.

There is a pronounced east-west gradient in summer surface temperature in the climatology, with warmer temperatures in the western half of the Gulf of Maine. The input of cold SSW in the eastern gulf is a tempting explanation for this gradient. However, Mountain and Manning (1994) have suggested that the timing of coastal runoff and its subsequent flooding of the western Gulf of Maine during spring/summer leads to enhanced water column stability and preferential trapping of heat at the surface. Moreover, due to the geometry of the basin and phasing of the seasonal cycle of temperature and salinity, the western half of the Gulf of Maine has a greater potential for deeper vertical mixing in winter and for stronger stratification in summer (Mountain and Manning, 1994). This leads to the horizontal temperature gradients that appear in the climatology, with the well-documented propensity for colder bottom waters in the deep western basins relative to the east (Taylor and Mountain, 2009).

Another notable signal in the climatological bottom temperature fields is the warm bottom temperature over Georges Bank and Nantucket Shoals due to strong tidal mixing. Garrett et al. (1978) showed that tidal mixing is strong enough to homogenize the water column over Georges Bank, Nantucket Shoals, in the Bay of Fundy and on the southwestern shore of Nova Scotia. This surely explains the fact that surface and bottom temperature and salinity are nearly identical in the eastern part of the Bay of Fundy. It could also play a role in the warming of bottom temperature off Nova Scotia.

If we take a closer look, we can see a surprising feature, which is the pool of very cold (<10 °C) water at the surface off Cape Sable Island, at the southern tip of Nova Scotia. Tee and Smith (1993) link it to a three-dimensional upwelling induced by strong tidal current, rather than a two-dimensional upwelling created by wind or estuarine-induced circulation. This upwelling is supposed to bring cold, saline and nutrient-rich water from deep to shallow regions, but surface salinity does not show a clearly delimited pool as does surface temperature.

5.4. Concluding remarks

Our dataset extends over more than 60 years and over a region of 25 degrees in latitude with a very high spatial resolution. To better understand the relationship between the surface and bottom temperature and salinity, it would be useful to add the mixed-layer depth to this dataset. In addition to the climatological seasonal cycle presented in this paper, our dataset will be useful to study the interannual variability of the surface and bottom temperature and salinity over the whole system, which will be the subject of a follow-up study. Our study clearly demonstrated the value of the long-term sustained observations and calls for a continued effort to enhance the regional and global observational network over the shelf, in parallel to the successful programs in the deep ocean, e.g. the Argo program, in particular considering the long-term changes already documented in these coastal regions (e.g. Shearman and Lentz, 2010; Chen et al., 2014; Forsyth et al., 2015; Loder and Wang, 2015).

Acknowledgements

We gratefully acknowledge the constructive reviews by Dr. Linda Rasmussen, an anonymous reviewer and the editor Dr. Matthew Palmer, and the support from NSF OCE PO to Y-OK (OCE-1242989 and OCE-1435602) and SJL (OCE-1332666). BR wish to thanks ENSTA ParisTech for allowing his secondment to WHOI.

References

Amante, C., B.W., Eakins, 2009. ETOPO1 1 Arc-Minute Global Relief Model: Procedures, Data Sources and Analysis. NOAA Technical Memorandum NESDIS NGDC-24. National Geophysical Data Center, NOAA. (09.09.2014).
Bourgault, D., Koutitonsky, V.G., 1999. Real-time monitoring of the freshwater discharge at the head of the St. Lawrence estuary. Atmos.-Ocean 37, 203–220.
Bigelow, H. B., 1933. Studies of the waters on the continental shelf, Cape Cod to Chesapeake Bay. I. The cycle of temperature. Papers in Physical Oceanography and Meteorology, vol. 2, pp. 1–135.
Chapman, D.C., Beardsley, R.C., 1989. On the origin of shelf water in the Middle Atlantic Bight. J. Phys. Oceanogr. 19, 384–391.
Chen, K., Gawarkiewicz, G., Kwon, Y.-O., Zhang, W.G., 2014. The role of atmospheric forcing versus ocean advection during the extreme warming on the Northeast U.S. shelf in 2012. J. Geophys. Res.
Deser, C., Holland, M., Reverdin, G., Timlin, M., 2002. Decadal variations in Labrador Sea ice cover and North Atlantic sea surface temperatures. J. Geophys. Res., 107.
Drinkwater, K.F., Gilbert, D., 2004. Hydrographic variability in the waters of the Gulf of St. Lawrence, the Scotian Shelf and the Eastern Gulf of Maine (NAFO Subarea 4) during 1991–2000. J. North. Atl. Fish. Sci. 34, 83–99.
Forsyth, J.S.T., Andres, M., Gawarkiewicz, G.G., 2015. Recent accelerated warming of the continental shelf off New Jersey: observations from the CMV Oleander expendable bathythermograph line. J. Geophys. Res. Ocean. 120, 2370–2384. http://dx.doi.org/10.1002/2014JC010516.
Frankignoul, C., de Coetlogon, G., Joyce, T.M., Dong, S.F., 2001. Gulf stream variability and ocean-atmosphere interactions. J. Phys. Oceanogr. 31, 3516–3529.
Fratantoni, P.S., McCartney, M.S., 2010. Freshwater export from the Labrador Current to the North Atlantic Current at the Tail of the Grand Banks of Newfoundland. Deep Sea Res., 57.
Fratantoni, P.S., Pickart, R.S., 2007. The Western North Atlantic shelfbreak current system in summer. J. Phys. Oceanogr. 37, 2509–2533.
Galbraith, P.S., 2006. Winter water masses in the Gulf of St. Lawrence. J. Geophys. Res. 111, C06022.
Garrett, C., Loder, J.W., 1981. Dynamical aspects of shallow sea fronts. Philos. Trans. R. Soc. Lond. A, 302.
Garrett, C.J.R., Keeley, J.R., Greenberg, D.A., 1978. Tidal Mixing versus thermal stratification in the Bay of Fundy and Gulf of Maine. Atmos.-Ocean 16, 403–423.
Gatien, M.G., 1976. A study in the Slope Water Region South of Halifax. J. Fish. Res. Board Can. 33, 2213–2217.
Gregory, D.N., 2004. Climate: A Database of Temperature and Salinity Observations for the Northwest Atlantic, DFO Can. Sci. Advis. Sec. Res. Doc. 2004/075.
Han, G., 2000. Three-dimensional modeling of tidal currents and mixing quantities over the Newfoundland Shelf. J. Geophys. Res. 105, 11407–11422.
Ikeda, M., Yao, T., Yao, Q., 1996. Seasonal evolution of sea ice cover and shelf water off Labrador simulated in a coupled ice-ocean model. J. Geophys. Res. 101, 16465–16489.
Khatiwala, S.P., Fairbanks, R.G., Houghton, R.W., 1999. Freshwater sources to the coastal ocean off northeastern North America: evidence from H218O/H216O. J. Geophys. Res. 104, 18241–18255.
Kipling, R., 1897. Captains Courageous, 2013 edition. Simon & Brown.
Li, Y., Fratantoni, P.S., Chen, C., Hare, J.A., Sun, Y., Beardsley, R.C., Ji, R., 2015. Spatio-temporal patterns of stratification on the Northwest Atlantic shelf. Prog. Oceanogr. 134, 123–137.
Loder, J.W., Wang, Z., 2015. Trends and variability of sea surface temperature in the Northwest Atlantic from three historical gridded datasets. Atmos.-Ocean, 1–19. http://dx.doi.org/10.1080/07055900.2015.1071237.
Loder, J.W., Petrie, B., Gawarkiewicz, G.G., 1998. The coastal ocean of northeastern North America: a large-scale view. The Sea: The Global Coastal Ocean Regional Studies and Syntheses 11. John Wiley & Sons, United States, pp. 3–27.
Loti, P., 1886. Pêcheur d'Islande. Le Livre de Poche.
Mountain, D.G., 2012. Labrador slope water entering the Gulf of Maine – response to the North Atlantic Oscillation. Cont. Shelf Res. 47, 150–155.
Mountain, D.G., Jessen, P.F., 1987. Bottom waters of the Gulf of Maine, 1978–1983. J. Mar. Res. 45, 319–345.
Mountain, D.G., Manning, J.P., 1994. Seasonal and interannual variability in the properties of the surface waters of the Gulf of Maine. Cont. Shelf Res. 14, 1555–1581.
National Ice Center, 2006. Compiled by F. Fetterer and C. Fowler. Updated 2009. National Ice Center Arctic Sea Ice Charts and Climatologies in Gridded Format. Boulder, Colorado USA, National Snow and Ice Data Center ⟨http://nsidc.org/⟩.
Peña-Molino, B., Joyce, T.M., 2008. Variability in the Slope Water and its relation to the Gulf Stream path. Geophys. Res. Lett. 35, L03606. http://dx.doi.org/10.1029/2007GL032183.
Petrie, B., 2007. Does the North Atlantic Oscillation affect hydrographic properties on the Canadian Atlantic Continental Shelf? Atmos.-Ocean 45, 141–151.
Rossby, T., Benway, R.L., 2000. Slow variations in mean path of the Gulf Stream east of Cape Hatteras. Geophys. Res. Lett. 27, 117–120.
Shearman, R.K., Lentz, S.J., 2010. Long-term sea surface temperature variability along the U.S. East Coast. J. Phys. Oceanogr. 40, 1004–1017.
Taylor, M.H., Mountain, D.G., 2009. The influence of surface layer salinity on wintertime convection in Wilkinson Basin, Gulf of Maine. Cont. Shelf Res. 29, 433–444.
Tee, K.T., Smith, P.C., 1993. Topographic Upwelling off Southwest Nova Scotia. J. Phys. Oceanogr. 23, 1703–1726.
Wu, Y., Tang, C., Hannah, C., 2012. The circulation of eastern Canadian seas. Prog. Oceanogr. 106, 28–48.
Xu, H., Kim, H.-M., Nye, J.A., Hameed, S., 2015. Impacts of the North Atlantic Oscillation on sea surface temperature on the Northeast US Continental Shelf. Cont. Shelf Res. 105, 60–66. http://dx.doi.org/10.1016/j.csr.2015.06.005.
Yu, L., Jin, X., Weller, R.A., 2008. Multidecadel global flux datasets from the Objectively Analyzed Air-sea Fluxes (OAFlux) Project: Latent and sensible heat fluxes, ocean evaporation, and related surface meteorological variables. Woods Hole Oceanographic Institution, OAFlux Project Tech. Rep. OA-2008-01, 64 pp (available online at ⟨http://oaflux.whoi.edu/⟩).